frontiers | Frontiers in Earth Science

TYPE Original Research
PUBLISHED 27 November 2025
DOI 10.3389/feart.2025.1634401

OPEN ACCESS

EDITED BY
Mounir Bouassida,
Tunis El Manar University, Tunisia

REVIEWED BY
Hongjian Zhu,
Yanshan University, China
Deendayal Rathod,
National Institute of Technology, India

*CORRESPONDENCE
Junyun Zhang,
zjywxfbb@swjtu.edu.cn

RECEIVED 03 June 2025
REVISED 13 October 2025
ACCEPTED 21 October 2025
PUBLISHED 27 November 2025

CITATION
Huang R, Wang B, Zhang L, Xiao D, Li B and Zhang J (2025) Model test study on rapid reinforcement technology for shallow soft foundations in sichuan basin.
Front. Earth Sci. 13:1634401.
doi: 10.3389/feart.2025.1634401

Model test study on rapid reinforcement technology for shallow soft foundations in sichuan basin

Rui Huang[1], Bo Wang[1], Le Zhang[1,2], Dong Xiao[3], Bing Li[2] and Junyun Zhang[1]*

[1]Southwest Jiaotong University, School of Civil Engineering, Chengdu, China, [2]Sichuan Highway Planning, Survey, Design and Research Institute Co., Ltd., Chengdu, China, [3]Chengdu Industrial Vocational and Technical College, Chengdu, China

Rapid reinforcement methods for shallow soft foundations are critical for guiding practical applications in subgrade engineering. This study uses model tests to examine how the particle size and number of compacted rock fill layers affect the reinforcement performance of shallow soft foundations. It analyzes the load-settlement behavior, key mechanical factors, and the long-term stability of the reinforced foundation. The results show that: (1) Foundation settlement decreases as the number of compacted layers increases, while both the ultimate bearing capacity and deformation modulus increase significantly. With layer counts rising from 0 to 1, 2, and 3, the bearing capacity improved by 113.27%, 47.91%, and 69.21% on average, while the deformation modulus increased by 39.54%, 12.16%, and 63.95% on average, depending on the rock fill size. Notably, using 9 cm rock fill and 3 compaction layers yielded a remarkable 709.83% increase in ultimate bearing capacity and a 329.17% increase in deformation modulus compared to the untreated foundation. (2) Both the ultimate bearing capacity and deformation modulus increase with higher maximum compacted stress. Empirical formulas were developed to predict bearing capacity and deformation mod-ulus, accounting for maximum compacted stress and particle size. Validation with experimental data showed that the formulas had an average relative error of less than 7.37%. (3) After an initial significant settlement increase (ranging from 76.03% to 208.29% at different points) due to the first rainfall saturation, the reinforced foundation remained stable, with minimal further impact (only 0.04%–2.15% additional settlement) from continued infiltration.

KEYWORDS

shallow soft foundation, model test, Reinforcement, compacted rock fil, ultimate bearing capacity

1 Introduction

Red beds, formed through Meso-Cenozoic continental sedimentation, are widely distributed in China. The Sichuan Basin, often referred to as the "Red Basin", is a key area for their concentrated presence (He et al., 2024; Wang and Shu, 2012). These rocks are typically weak and classified as soft due to their short depositional history

and low levels of diagenesis. They exhibit low permeability and high hydrophilicity, leading to water-induced softening and disintegration upon drying (He et al., 2025). These properties contribute to common foundation isses such as low bearing capacity, surface instability, and settlement cracking (Zhang et al., 2024; Zhu J. et al., 2025) reinforcement essential for improving mechanical performance and ensuring stability.

Various engineering solutions have been proposed to reinforce shallow soft foundations. Traditional methods include replacement, dynamic compaction, composite foundations, deep mixing, and vacuum preloading (Zhang et al., 2021; Zhou S. et al., 2020) stabilization, which forms hard crust layers, is commonly used in European engineering practice. However, research (Wang et al., 2021; Zhou D. et al., 2020) at meeting bearing capacity standards alone is not enough for road projects with strict settlement criteria, in comparison, DM piles and prefabricated vertical drains have become the most commonly used ground improvement techniques for embankment construction on soft soils (Rujikiatkamjorn et al., 2008; Liu et al., 2012; Shen et al., 2013). Cheng et al. (2015) found that high and low-liquid-limit clays had volume compression rates of 47.4% and 22.9%, respectively, demonstrating the critical role of soil properties in reinforcement outcomes. He and Li (2019) and Lei et al. (2020) showed that vacuum preloading with surcharge loading enhanced soil strength most at 15–20 m depths, but did not resolve thixotropic behavior. Deep mixing techniques, which use cement or lime-based agents, strengthen foundations (Pan et al., 2022; Wang et al., 2023); Rao et al. (2024) developed reinforced columns that show promise for deep soft soils, Nguyen and Nguyen (2020), Nguyen and Nguyen (2018) employed the finite element method (PLAXIS software) to investigate the stress distribution in soft ground reinforced by CDM (Cement Deep Mixing) piles combined with geotextiles in embankment projects. Ren et al. (2021) and Li et al. (2021) highlighted the distinctive benefits of electro-osmosis for reinforcing soft clay.

Despite theoretical progress, practical challenges remain in treating shallow soft foundations. Technique selection must consider site conditions, construction schedules, and cost efficiency. Comparative studies reveal key limitations: dynamic compaction generates strong vibrations (Feng et al., 2021; Sun et al., 2025); grouting is costly and geologically constrained (Su et al., 2023); and composite foundations are time-consuming and expensive (Hu, 2021). Crucially, three research gaps remain unaddressed: Lack of rapid solutions for shallow red beds (<2 m depth) requiring short construction cycles; Absence of economical techniques utilizing locally abundant rock materials; Insufficient quantitative models correlating compaction parameters with bearing capacity enhancement (Chi et al., 2024; Office et al., 2021). In response, this study proposes a rapid reinforcement method using compacted rock fill, based on the replacement approach and tailored for shallow red bed foundations in the Sichuan Basin (Zhou et al., 2020). This method leverages locally abundant rock fill material, minimizing material costs (Yang et al., 2025). The construction process involves simple layered placement and compaction, significantly reducing time compared to techniques requiring curing (e.g., cement-based methods) or complex installation (e.g., drains or piles). Crucially, it generates minimal vibration compared to dynamic compaction (Devahi et al., 2022a). Its efficiency, economy, and suitability for shallow applications make it well-adapted to the regional engineering conditions."

The primary objectives of this study are to: (1) Quantitatively evaluate how rock fill particle size (6/9/12 cm) and compaction layer number (0–3 layers) affect the ultimate bearing capacity and deformation modulus of shallow soft foundations (Devahi et al., 2023); (2) Establish empirical models predicting bearing capacity and deformation modulus based on maximum compaction stress and particle size; (3) Assess long-term stability under repeated saturation cycles. We hypothesize that: An optimal particle size (9 cm) exists for maximizing reinforcement efficiency (Devahi et al., 2022b); Increasing compaction layers will nonlinearly improve mechanical properties; Water-induced settlement will stabilize after initial saturation.

2 Model test

Field testing is often limited by challenging site conditions and the high cost of labor and materials. Scaled physical model testing offers a cost effective and efficient alternative for engineering research. This study develops a physical model based on similarity principles, using precise instrumentation to maintain controlled boundary conditions (Zhu H. et al., 2025). It systematically investigates the mechanical behavior of compacted rock fill reinforcement in soft foundations, emphasizing strength development and deformation behavior of the composite foundation (Yang et al., 2024). A key consideration for field application is the scale effect. While adhering to fundamental similarity principles ($C\gamma = C\varphi = Cc = C\mu = 1{:}1$), geometric scaling (CL = 5:1) simplifies complex field interactions. Prototype rock properties (e.g., angularity) are challenging to scale perfectly, and boundary effects in the test tank differ from the semi-infinite natural subgrade. Consequently, while the model tests reliably identify optimal parameters (e.g., 9 cm model size ≈45 cm prototype) and qualitative trends, direct quantitative extrapolation of absolute values (e.g., settlement) requires caution. The empirical formulas are most valuable for predicting relative improvement and guiding preliminary field design. The objectives of the tests are to:

1. Develop selection criteria for rock fill based on optimal particle gradation.
2. Assess the engineering feasibility of the compaction process for reinforcing soft foundations.
3. Quantify the relationship between compaction quantity and the foundation's bearing capacity and deformation modulus.
4. Evaluate the long-term performance of the reinforced foundation.

2.1 Prototype generalization and similarity ratio design

Geotechnical data from the K66 + 080–K66 + 321 section of a highway project show that the weak foundation consists mainly of soft-plastic silty clay (1.4–1.7 m thick, averaging 1.5 m), overlying highly weathered red bed soft rock. The model replicates this profile with a dual-layer structure: a 1.5 m-thick upper layer of soft-plastic silty clay and an underlying red bed soft rock base. Key physical and mechanical properties of the silty clay are summarized

TABLE 1 Key physical and mechanical parameters of soft-plastic silty clay.

Soil/rock name	State	Unit weight (kN/m^3)	Water content (%)	Void ratio	Compression modulus (Mpa)	Poisson's ratio	Internal friction angle (°)	Cohesion (kPa)
Silty clay	Soft-plastic	19.0	32.3	0.89	2.8	—	9.7	10.1
Red bed soft rock		23.0	—	—	—	—	—	—

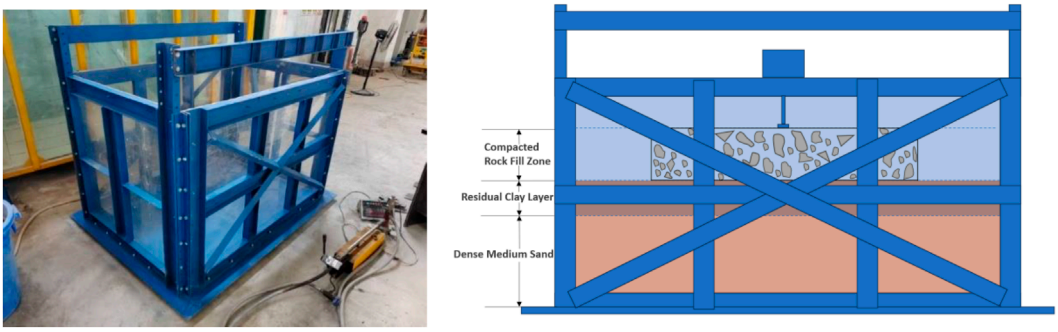

FIGURE 1
Test tank.

in Table 1. Figure 1 shows the test tank used in the experiment. A geometric similarity ratio of CL = 5:1 was adopted based on similarity theory. A custom model test system was constructed with internal dimensions of 1.5 m × 1.25 m × 1.0 m. The test tank includes a rigid base made of an 8 mm-thick Q235 steel plate. The sidewalls consist of a channel steel frame with 10 mm-thick plexiglass panels. Rubber water stop were added at joints, and the tank was assembled modularly using high-strength bolts.

2.2 Test materials

2.2.1 Simulation of geotechnical media

Based on representative stratigraphic features, the test simulated two geotechnical materials: soft-plastic silty clay and red bed soft rock. The model strictly followed similarity principles, applying key similarity ratios: unit weight Cγ = 1:1, deformation CE = 1:1, Poisson's ratio Cμ = 1:1, and strength parameters Cc = 1:1, Cφ = 1:1. The following methods were used to simulate the materials:

1. Red bed soft rock: Simulated with medium sand, placed in layers at the bottom of the tank. After compaction to achieve a dense state, the sand was saturated with water to form a 40 cm thick layer.
2. Soft-plastic silty clay: Simulated using remolded clay prepared by adding water to reach a fluid-plastic state, then compacted in layers. The shear strength normal stress curve and the e–p curve are shown in Figures 2, 3, with key parameters listed in Table 2.

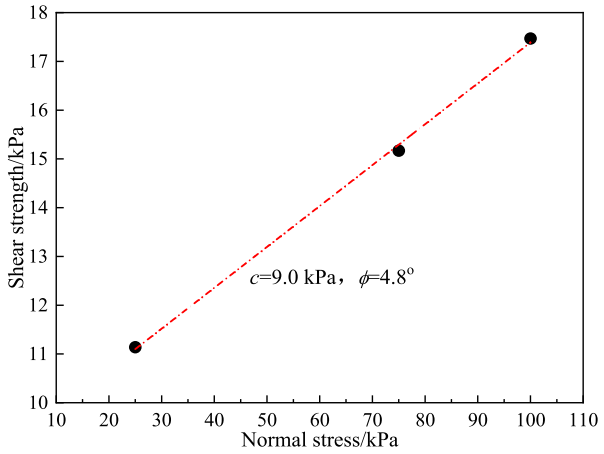

FIGURE 2
Shear strength envelope of tested soil.

2.2.2 Compacted rock fill materials

In the prototype design, rock fill of 30 cm, 45 cm, and 60 cm particle sizes was used. For the model test, these sizes were scaled down to 6 cm, 9 cm, and 12 cm granite blocks (Figure 4) according to the geometric similarity ratio CL = 5. Critical parameters such as compressive strength and surface roughness of the rock fill were calibrated to match the similarity criteria.

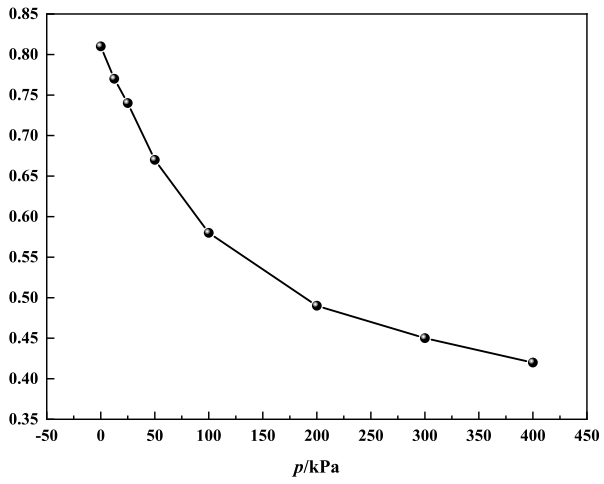

FIGURE 3
e-p curve of tested soil.

2.3 Loading and measurement systems

The loading system for the compacted rock fill is shown in Figure 5a. A hydraulic jack, positioned at the center of a 30 cm × 30 cm steel plate, applied the load. Force measurements were obtained using a load cell integrated with a reaction beam, with data collected via a high-precision digital readout device (minimum resolution: 1 kg, equivalent to 0.57 kPa).

The foundation bearing capacity testing system (Figure 5b) uses a 15 cm-diameter circular steel plate. Loads are applied using a hydraulic jack, with load settlement data recorded in real time. The measurement resolution is 1 kg, corresponding to an applied stress of 0.57 kPa. Settlement was monitored using symmetrically positioned dial indicators with an accuracy of ±0.01 mm.

2.4 Test scheme

Three sets of compaction tests were conducted using rock fill with particle sizes of 6 cm, 9 cm, and 12 cm. The procedure included: (1) Model preparation, a 40 cm-thick water-saturated, densely compacted medium sand layer was constructed, overlaid by a 30 cm-thick uniformly mixed fluid-plastic clay layer within the test tank. (2) Initial plate load testing, baseline measurements of bearing capacity and deformation modulus of the clay foundation were taken at three central points in accordance with JTG D63-2007 standards. (3) Layered compaction, rock fill of varying particle sizes was compacted in layers, maintaining a 30 cm buffer from the tank walls. Plate load tests were conducted after each compaction layer (Figures 6a,b). (4) Long-term settlement monitoring (9 cm group only), a 50 cm-thick fill layer was installed with four measurement points. Two saturation cycles were performed (initial and secondary) to evaluate stabilization and capture settlement data.

3 Analysis of compaction test results

3.1 Compaction load-foundation settlement curves

Settlement response characteristics under compaction loads are illustrated in Figure 7. The test results show that foundation settlement is strongly positively correlated with compaction load. The rate of increase is influenced by the interaction between the number of compaction layers and rock fill particle size. Specifically: Influence of Layer Number: For a constant load and particle size, settlement decreases with increasing compaction layers. At 14 kPa, the 9 cm particle group showed average settlements at Point 1 of 4.01 mm (3 layers), 0.70 mm (2 layers), 0.48 mm (1 layer), and 0.18 mm (0 layers). Sensitivity to Particle Size: With one or more compaction layers, settlement varied by particle size. The 9 cm group exhibited the least settlement, followed by 12 cm, while the 6 cm group resulted in the highest settlement.

Based on the data in Figure 7, essential mechanical parameters were derived using shallow plate load tests (see Table 3): Ultimate Bearing Capacity: Defined according to JTG D63-2013 as the load at which the settlement to plate diameter ratio reaches 0.06, equivalent to 9 mm for a 15 cm loading plate. Maximum Compaction Stress: Calculated as the peak load required to penetrate the rock fill divided by the area of the square loading plate. Deformation Modulus: Calculated from the initial linear portion of the p–s curve, based on the theory of a homogeneous, isotropic, semi-infinite elastic medium (Equation 1).

$$E_0 = I_0(1-\mu^2)\frac{pd}{s} \tag{1}$$

Where: E_0 = deformation modulus of the foundation (Mpa); I_0 = shape factor (0.785 for circular plates, 0.866 for square); μ^2 = Poisson's ratio; d = plate diameter or side length (m); p = pressure in the linear segment (kPa); s = corresponding settlement (mm).

3.2 Analysis of factors influencing the mechanical properties of soft foundations

3.2.1 Effect of compaction layers on the mechanical properties of soft foundations

Figure 8 illustrates the evolution of the ultimate bearing capacity of shallow soft foundations with increasing layers of compacted rock fill. The results demonstrate a significant nonlinear improvement in bearing capacity with additional compaction layers. For instance, when using 9 cm rock fill, the ultimate bearing capacity increased by 200.58%, 343.93%, and 709.83% as the number of compaction layers increased from 0 to 1, 2, and 3, respectively. This enhancement occurred in a nonlinear manner: the largest average increase (113.27%) occurred between 0 and 1 layer, followed by a slower growth rate of 47.91% from 1 to 2 layers, and a subsequent rebound to 69.21% between 2 and 3 layers. This trend underscores the complex interaction between compaction layers and rock fill particles in influencing mechanical behavior.

TABLE 2 Key physical and mechanical parameters of geotechnical materials in model tests.

Soil/rock name	State	Unit weight (kN/m^3)	Water content (%)	Void ratio	Compression modulus (Mpa)	Poisson's ratio	Internal friction angle (°)	Cohesion (kPa)
Clay	Fluid-plastic	19.0	32.3	0.81	1.7	—	4.8	9.0
Medium sand	Dense	20.5	—	0.62	36	—	35	—

FIGURE 4
Compacted rock fill materials. **(a)** Rock fill particle size: 6 cm. **(b)** Rock fill particle size: 9 cm **(c)** Rock fill particle size: 12 cm.

FIGURE 5
Loading and measurement system.

Normalized results in Figure 8 further confirm the reinforcement effectiveness. For example, compacted rock fill using 12 cm particles improved ultimate bearing capacity by over 67.68% relative to untreated foundations. These findings affirm the practical efficacy of layered compaction in rapidly enhancing load-bearing performance, particularly in applications requiring stringent control of settlement.

In addition to increased bearing capacity, the deformation modulus of the foundation also improves with additional compaction layers. As shown in Figure 9, the deformation modulus follows a trend similar to that of the ultimate bearing capacity. For example, in the 9 cm rock fill group, the deformation modulus increased by 115.28%, 131.94%, and 329.17% as the number of layers increased from 0 to 1, 2, and 3, respectively, normalized to the untreated condition. Notably, a minimal gain was observed between 1 and 2 layers, echoing the nonlinear pattern seen in bearing capacity. For the 6 cm and 12 cm rock fill groups, however, the deformation modulus showed a more consistent incremental trend with each additional layer. Specifically, the 6 cm group achieved relative increases of 3.33%, 25.00%, and 103.33% for 0→1, 1→2, and 2→3 layers, respectively.

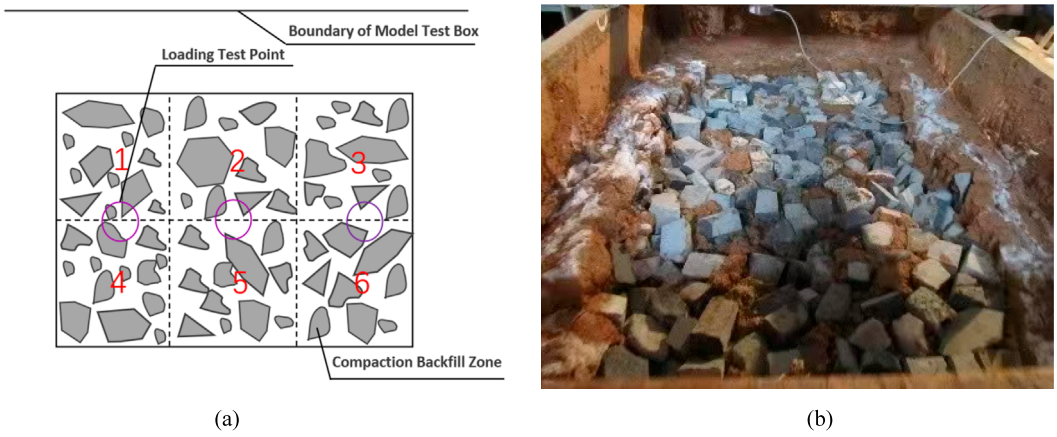

FIGURE 6
Compaction test scheme. **(a)** Compaction sequence. **(b)** Compaction effect of rock fill.

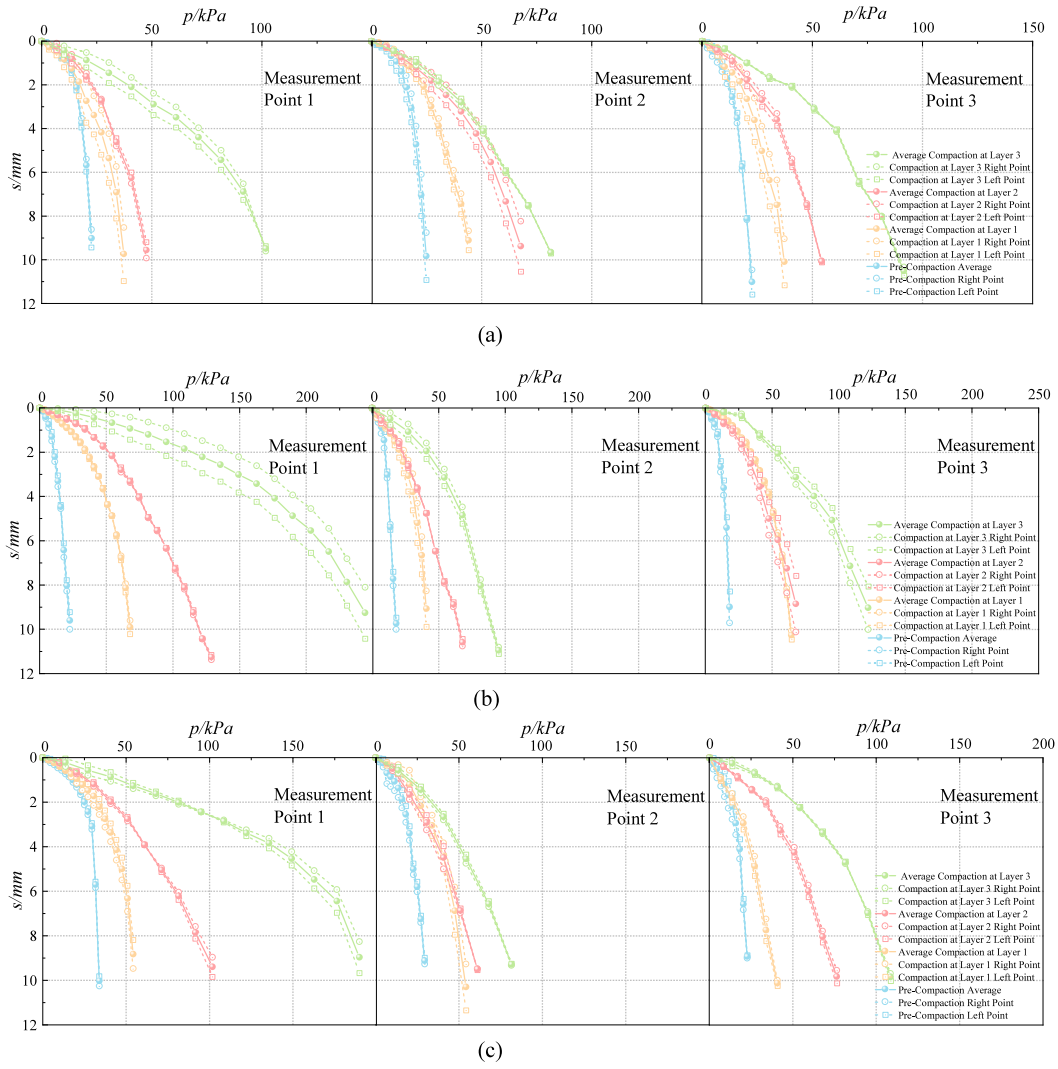

FIGURE 7
p-s curves. **(a)** Rock fill particle size: 6 cm. **(b)** Rock fill particle size: 9 cm. **(c)** Rock fill particle size: 12 cm.

TABLE 3 Summary of compaction test results.

D/mm	Compaction layers	Ultimate bearing capacity/kPa				Deformation modulus/Mpa				Maximum compaction stress/kPa
		Point 1	Point 2	Point 3	Average	Point 1	Point 2	Point 3	Average	
6	0	20.30	22.60	20.30	21.10	1.21	1.13	0.75	1.03	—
	1	33.90	40.70	33.90	36.20	1.06	1.20	0.83	1.03	34.10
	2	40.70	61.00	47.50	49.70	1.15	1.30	0.87	1.11	56.80
	3	91.50	71.20	81.40	81.40	1.65	1.38	1.78	1.60	71.70
9	0	20.30	15.80	15.80	17.30	0.65	0.77	0.73	0.72	—
	1	61.00	37.30	57.60	52.00	1.82	1.06	1.77	1.55	38.30
	2	108.50	61.00	61.00	76.80	2.40	1.01	1.59	1.67	62.80
	3	230.50	81.40	108.50	140.10	5.47	2.02	1.78	3.09	90.50
12	0	31.60	27.10	20.30	26.30	1.94	0.91	0.75	1.20	—
	1	50.80	47.50	33.90	44.10	1.88	1.15	0.68	1.24	31.10
	2	91.50	50.80	67.80	70.00	1.93	0.96	1.61	1.50	50.10
	3	176.30	67.80	94.90	113.00	3.62	1.45	2.25	2.44	74.90

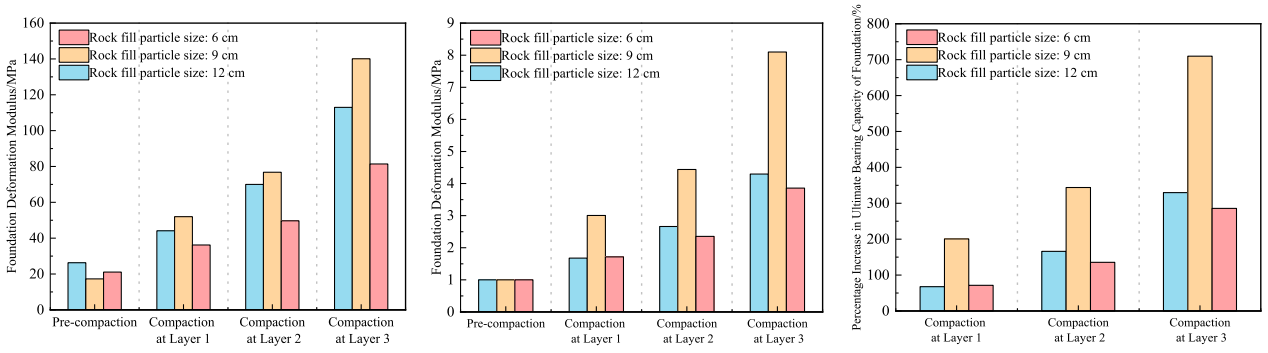

FIGURE 8
Effect of compaction layers on the ultimate bearing capacity of shallow foundations.

3.2.2 Effect of rock fill particle size

Rock fill particle size significantly affects the mechanical response of reinforced foundations. Across one to three compaction layers, the 9 cm rock fill group consistently delivered the highest ultimate bearing capacity (140.10 kPa) and deformation modulus (3.09 MPa), followed by the 12 cm group (113.00 kPa, 2.44 MPa), with the 6 cm group performing the least effectively (81.40 kPa, 1.60 MPa). These results suggest that the relationship between particle size and mechanical performance is not linear. Instead, an optimal particle size (e.g., 9 cm) exists that maximizes reinforcement effectiveness, while deviations from this size result in diminished performance.

Further analysis shown in Figure 7 confirms that the 9 cm group exhibited the highest overall improvement under three compaction layers, achieving increases of 74.08% in ultimate bearing capacity and 76.70% in deformation modulus compared to untreated foundations. In contrast, the 6 cm and 12 cm groups achieved relatively lower gains (e.g., 35.63% and 50.82% improvement in deformation modulus, respectively).

3.2.3 Effect of maximum compaction stress

Figure 10 reveals a strong exponential correlation between the maximum compaction stress (i.e., the stress required to embed

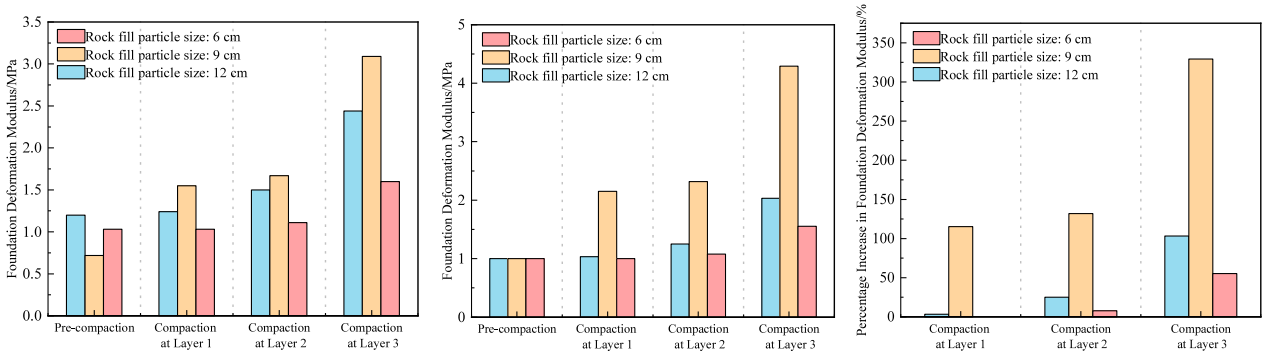

FIGURE 9
Effect of compaction layers on the deformation modulus of shallow foundations.

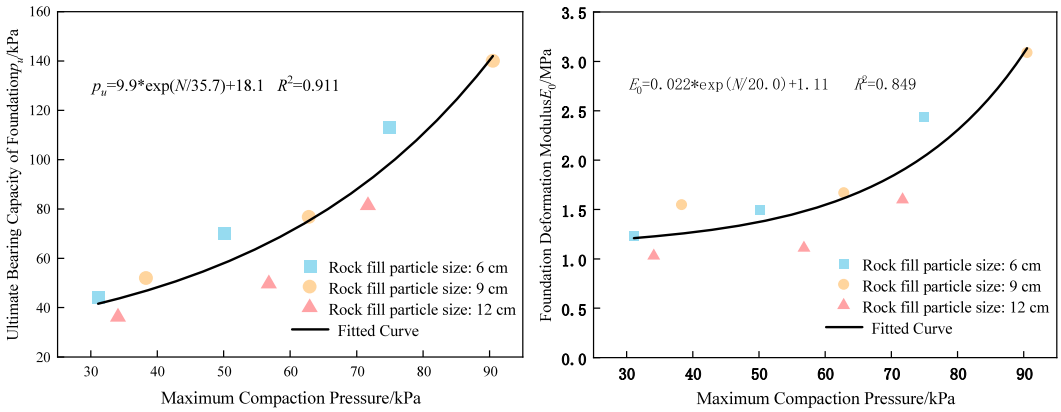

FIGURE 10
Effect of maximum compaction stress on the mechanical properties of soft foundations.

rock fill) and the ultimate bearing capacity of the foundation. This relationship is expressed by Equation 2, with a high coefficient of determination (R^2 = 0.911), indicating that increased compaction stress significantly contributes to the foundation's load-bearing enhancement, particularly for fills with uniform particle size distribution.

$$Pu = 9.9 \cdot e^{(N/35.7)} + 18.1 \quad (2)$$

The calculated ultimate bearing capacities for soft foundations reinforced with rock fill particle sizes of 6 cm, 9 cm, and 12 cm yielded average relative errors of 11.50%, 4.39%, and 22.71%, respectively, when compared to experimental values. These findings emphasize the necessity of accounting for particle size effects in the predictive modeling of ultimate bearing capacity.

Moreover, while the relationship between maximum compaction stress and ultimate bearing capacity remains strongly positive, the influence of particle size on the growth trend of bearing capacity is minimal. That is, increasing particle size does not significantly alter the general evolution pattern of bearing capacity with compaction stress. To better capture the impact of particle size, the constant term in the original exponential fitting equation was replaced with a particle size dependent variable, resulting in a revised formula:

$$Pu = 9.9 \cdot e^{(N/35.7)} + \frac{N^{0.3}}{1.5} D \quad (3)$$

Figure 11 compares the results predicted by this refined formula (Equation 3) with experimental data. Except for the 6 cm rock fill group under a maximum compaction stress of 56.80 kPa, which showed a relatively large prediction error of 24.82%, all other cases exhibited prediction errors below 10%. The overall average relative error across all test conditions was 7.37%, indicating high predictive accuracy of the revised model.

In addition to bearing capacity, maximum compaction stress also exerts a significant influence on the deformation modulus of the soft foundation. As illustrated in Figure 11, the deformation modulus increases positively with maximum compaction stress. This relationship was initially fitted using an exponential function (Equation 4).

$$E_0 = 0.022 \cdot e^{(N/20)} + 11.1 \quad (4)$$

However, the resulting average relative errors between predicted and experimental values were 8.83% for the 6 cm group, 7.83% for the 9 cm group, and 24.13% for the 12 cm group. The relatively high

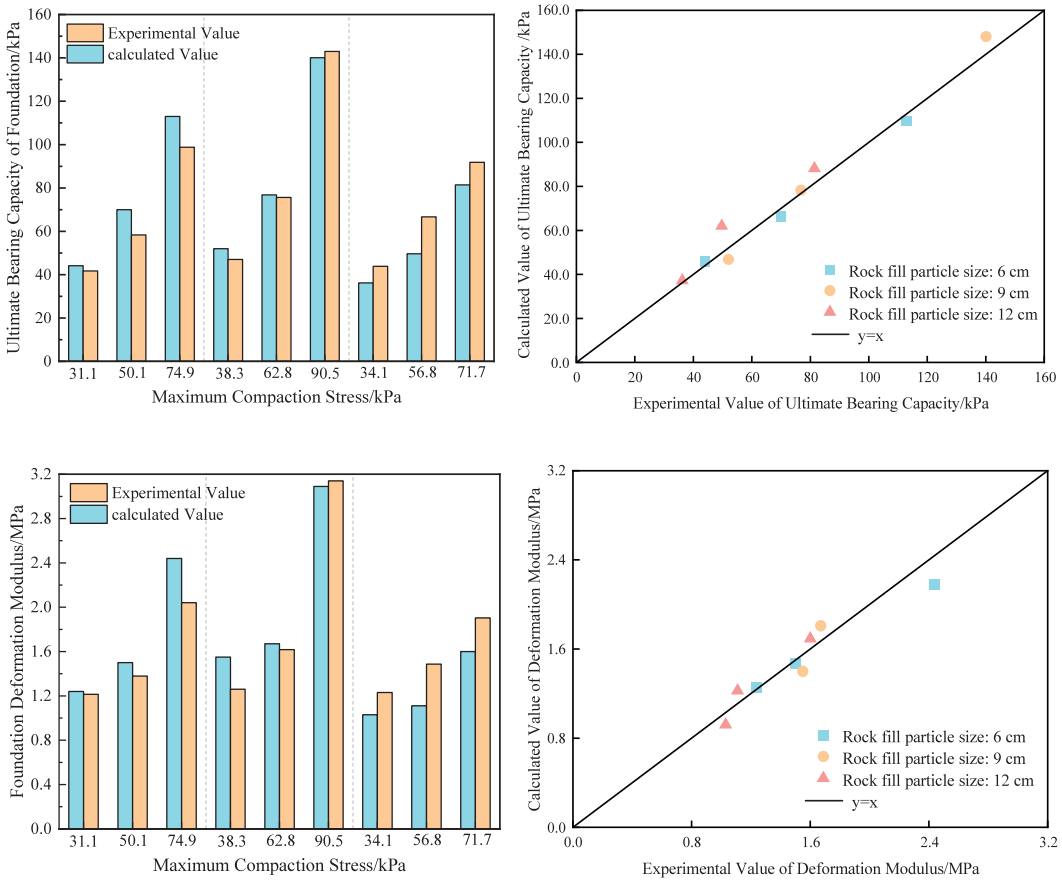

FIGURE 11
Comparison of formula predictions.

error for the 12 cm group indicates that particle size also plays a critical role in deformation behavior and should be incorporated into the predictive model. To address this, the deformation modulus equation was similarly refined by introducing a particle size dependent term into Equation 4, yielding an improved formulation.

$$E_0 = 0.022 \cdot e^{(N/20)} + 0.0003 \cdot D^2 \cdot L - 0.0044 \cdot D \cdot L + 0.042 \cdot L - 0.03 \cdot D^2 + 0.606 \cdot D - 1.91 \quad (5)$$

$$L = \sqrt{N} \quad (6)$$

Figure 11 presents the comparison between calculated results using the refined formula (Equations 5, 6) and experimental measurements. All prediction errors were maintained below 10.56%, with average relative errors of 5.79%, 9.21%, and 8.18% for the 6 cm, 9 cm, and 12 cm rock fill groups, respectively. These results confirm the improved formula's strong predictive performance across varying particle sizes.

4 Analysis of compaction test results

To assess the long-term stability of the composite foundation reinforced using compacted rock fill, a settlement monitoring program was implemented for the model test using 9 cm rock fill. The procedure included: Fill Layer Construction: A 50 cm-thick soil layer was compacted atop the composite foundation to replicate pavement loading conditions. Four settlement gauges were installed at designated locations within the model tank. Initial Settlement Monitoring: Subgrade settlement was continuously observed for 14 days following fill placement, with measurements taken until stabilization was achieved. First Saturation Cycle: The tank was saturated to mimic significant rainfall infiltration. Settlement data were collected over 12 days until settlement stabilized. Second Saturation Cycle: The flooding procedure was repeated to examine the impact of recurring rainfall or wetting-drying cycles on settlement progression.

The long-term settlement behavior of the reinforced foundation is illustrated in Figure 12, which delineates three distinct phases: static stabilization, initial water saturation, and secondary water saturation. Key findings are summarized below: Static Stabilization Phase: Following the placement of the 50 cm fill layer, the foundation exhibited gradual settlement stabilization over a 14-days period. Settlement increments progressively decreased, with final values of 2.33 mm, 3.95 mm, 2.39 mm, and 1.42 mm at points 1 through 4. The settlement time curves trended toward horizontal asymptotes, indicating stabilization. Initial Water Saturation Phase: Upon water infiltration, sharp increases in settlement were observed on the

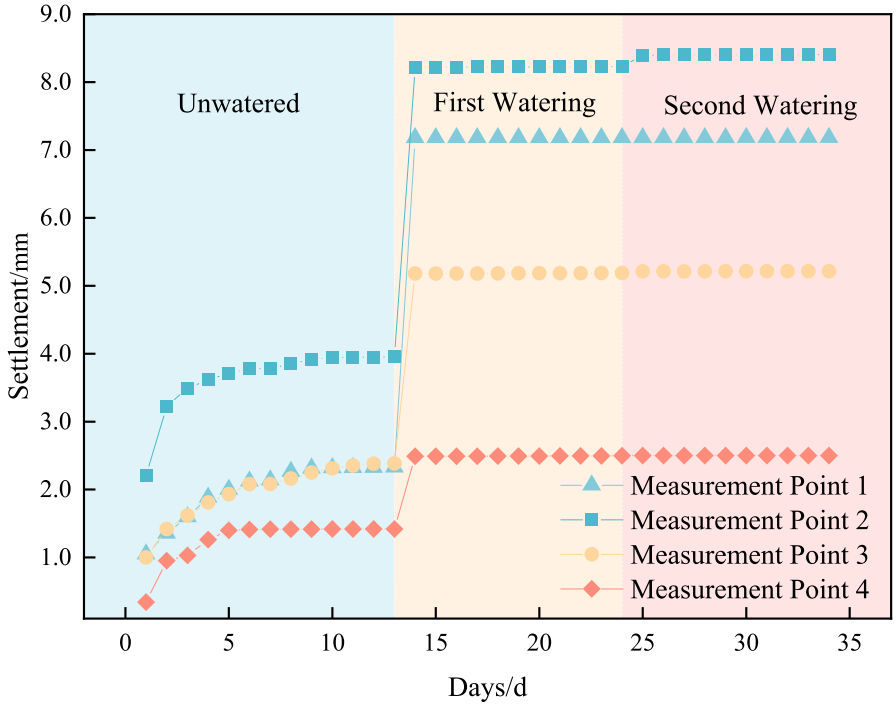

FIGURE 12
Long-term stability data.

first day, followed by rapid stabilization. Final settlements increased to 7.18 mm, 8.23 mm, 5.19 mm, and 2.50 mm at points 1–4, representing rises of 208.29%, 108.15%, 117.44%, and 76.03%, respectively, over the static phase. The curves showed an abrupt upward shift, then leveled off. Secondary Water Saturation Phase: A second saturation cycle caused only minor additional settlement. Final values at points 1–4 reached 7.18 mm, 8.41 mm, 5.22 mm, and 2.50 mm, representing increases of just 0.04%, 2.15%, 0.52%, and 0.12% over the initial saturation phase, respectively.

5 Conclusion

This study systematically explored the effects of varying rock fill particle sizes and compaction layer configurations on the mechanical behavior of soft foundations through indoor model tests. The key findings are summarized below:

1. Under consistent particle size and external loading, foundation settlement decreased with more compaction layers, while both ultimate bearing capacity and deformation modulus increased:

When compaction layers increased from 0 to 1, 2, and 3, the average increases in ultimate bearing capacity were 113.27%, 47.91%, and 69.21%, respectively; Corresponding increases in deformation modulus were 39.54%, 12.16%, and 63.95%, respectively.

1. An optimal rock fill particle size of 9 cm yielded the highest enhancement in bearing capacity and deformation modulus. Particle sizes smaller (6 cm) or larger (12 cm) led to diminished performance, suggesting nonlinearity and the importance of size optimization.
2. The ultimate bearing capacity and deformation modulus showed strong positive correlations with maximum compaction stress. Revised empirical formulas accounting for both stress and particle size achieved high predictive accuracy, with average relative errors below 7.37%.
3. Significant settlement occurred only during the initial water infiltration phase. Subsequent wetting events resulted in negligible additional deformation, confirming the excellent long-term stability of soft foundations reinforced by compacted rock fill.

Data availability statement

The original contributions presented in the study are included in the article/supplementary material, further inquiries can be directed to the corresponding author.

Author contributions

RH: Writing – original draft, Writing – review and editing. BW: Writing – original draft, Writing – review and editing. LZ: Writing – original draft, Writing – review and editing. DX: Writing – original draft, Writing – review and editing. BL: Writing – original draft,

Writing – review and editing. JZ: Writing – original draft, Writing – review and editing.

Funding

The author(s) declare that no financial support was received for the research and/or publication of this article.

Conflict of interest

Authors LZ and BL were employed by Sichuan Highway Planning, Survey, Design and Research Institute Co., Ltd.

The remaining authors declare that the research was conducted in the absence of any commercial or financial relationships that could be construed as a potential conflict of interest.

Generative AI statement

The author(s) declare that no Generative AI was used in the creation of this manuscript.

Any alternative text (alt text) provided alongside figures in this article has been generated by Frontiers with the support of artificial intelligence and reasonable efforts have been made to ensure accuracy, including review by the authors wherever possible. If you identify any issues, please contact us.

Publisher's note

References

Cheng, J., Zhang, Y., Zhang, Q., and Zhang, Y. (2015). Model experimental study on the applicability of vacuum preloading to treat high liquid limit clay. *Port and Waterw. Eng.* 40 (11), 155–159. doi:10.16233/j.cnki.issn1002-4972.2015.11.030

Chi, Y., Xiao, H., Zhang, Z., Wang, Y., Qian, Z., and Zhao, W. (2024). Influence of wind-blown sand content on the mechanical quality state of ballast bed in sandy railways. *Railw. Eng. Sci.* 32 (04), 533–550. doi:10.1007/s40534-024-00343-7

Devahi, P., Rathod, D., and Muthukkumaran, K. (2022a). Sustainable reuse potential of landfill mining waste retrieved from urban mining sites in South India. *J. Material Cycles Waste Manag.* 24 (6), 2582–2597. doi:10.1007/s10163-022-01506-6

Devahi, P., Rathod, D., and Muthukkumaran, K. (2022b). Building material synthesization using municipal solid waste incineration ash: a state-of-the-art review. *Environ. Technol. Rev.* 11 (1), 33–48. doi:10.1080/21622515.2021.2024890

Devahi, P., Rathod, D., and Muthukkumaran, K. (2023). Characterisation of soil-like material restored from landfill mining activities in Indian cities. *Aus J. Civ. Eng.*, 1–10. doi:10.1080/14488353.2023.2192022

Feng, S., Lei, H., Wang, L., and Hao, Q. (2021). The reinforcement analysis of soft ground treated by thermal consolidation vacuum preloading. *Transp. Geotech.* 31, 100672. doi:10.1016/j.trgeo.2021.100672

He, C., and Li, J. (2019). Experimental study on treatment of deep soft soil by preloading combined with vacuum. *Geotech. Eng. Tech.* 33 (2), 115–120. doi:10.3969/j.issn.1007-2993.2019.02.013

He, Z., Zhang, J., Luo, X., Huang, R., Yang, T., and Wu, X. (2024). A 3D DEM modeling of soil-rock mixture considering spatial distribution orientation of blocks. *Sci. Rep.* 14 (1), 25647. doi:10.1038/s41598-024-77366-x

He, Z., Zhang, J., Luo, X., Zhang, L., and Yang, T. (2025). Particle crushing behavior and strength generation mechanism of red-bed soil-rock mixture. *J. Southwest Jiaot. Univ.*, 1–11. doi:10.3969/j.issn.0258-2724.20230636

Hu, Z. (2021). "Experimental study on flocculation-vacuum-electroosmosis method for strengthening soft soil foundation in coastal area," 6th International Conference on Hydraulic and Civil Engineering, ICHCE 2020. doi:10.1088/1755-1315/643/1/012167

Lei, S., Liu, H., Liu, K., and Luo, Y. (2020). Effectiveness analysis of submerged vacuum preloading method for soft ground improvement. *For. Eng.* 36 (6), 95–102. doi:10.16270/j.cnki.slgc.2020.06.013

Li, W., Liu, W., Shen, M., Sun, X., and Li, Z. (2021). Effects of applied voltage and concentration of chemical solution on the electro-osmotic consolidation of kaolin. *Int. J. Electrochem. Sci.* 16 (12), 211215. doi:10.20964/2021.12.01

Liu, S. Y., Du, Y. J., Yi, Y. L., and Puppala, A. J. (2012). Field investigations on performance of T-shaped deep mixed soil cement column-supported embankments over soft ground. *J. Geotechnical Geoenvironmental Eng.* 138 (6), 718–727. doi:10.1061/(asce)gt.1943-5606.0000625

Nguyen, N. T., and Nguyen, A. T. (2018). Nonlinear FEM analysis of cement column configuration in the foundation improved by deep mixing method. *Strength Mater. Theory Struct.* 100, 1826.

Nguyen, A. T., and Nguyen, N. T. (2020). Study on stress distribution in soft ground consolidated with deep cement mixing columns under road embankment. *Civ. Eng. Archit.* 8 (6), 1251–1265. doi:10.13189/cea.2020.080609

Office, E. J., Chen, J., Dan, H., Gao, Y., Guo, M., Guo, S., et al. (2021). New innovations in pavement materials and engineering: a review on pavement engineering research 2021. *J. Traffic Transp. Eng. Ed.* 8 (06), 815–999. doi:10.1016/j.jtte.2021.10.001

Pan, H., Tong, L., Wang, Z., and Yang, T. (2022). Effects of deep soil mixing on existing shield tunnels in soft soil ground. *Undergr. Space* 7 (4), 724–733. doi:10.1016/j.undsp.2021.12.004

Rao, F., Xu, Y., Zhang, Z., Ye, G., and Chen, T. (2024). Analytical solution for consolidation of soft soil with partially penetrated stiffened deep-mixed columns under an embankment. *Int. J. Geomechanics* 24 (6), 04024084. doi:10.1061/ijgnai.gmeng-9281

Ren, L., Cao, H., and Kong, G. (2021). Experimental study on the effect of injection position on soft clay reinforcement by chemical-electroosmosis method. *Rock Soil Mech.* 42 (10), 2705–2712, 2721. doi:10.16285/j.rsm.2021.0116

Rujikiatkamjorn, C., Indraratna, B., and Chu, J. (2008). 2D and 3D numerical modeling of combined surcharge and vacuum preloading with vertical drains. *Int. J. Geomechanics* 8 (2), 144–156. doi:10.1061/(asce)1532-3641(2008)8:2(144)

Shen, S. L., Wang, Z. F., Sun, W. J., Wang, L. B., and Horpibulsuk, S. (2013). A field trial of horizontal jet grouting using the composite-pipe method in the soft deposits of shanghai. *Tunn. Undergr. Space Technol.* 35, 142–151. doi:10.1016/j.tust.2013.01.003

Su, D., Song, Q., Lin, X., and Chen, X. (2023). Limit equilibrium models for active failures of large-diameter shield tunnel faces in soft clay reinforced with soil–cement walls. *Comput. Geotechnics* 153, 105104. doi:10.1016/j.compgeo.2022.105104

Sun, Y., Zhan, J., Lu, Q., Zhu, W., and Peng, J. (2025). Spatiotemporal evolution and strategies for breaking the land subsidence and ground fissures disaster chain within the context of rapid urbanization[J/OL]. *J. Earth Sci.* 1–32. doi:10.13544/j.cnki.jeg.2022-0140

Wang, D., and Shu, L. (2012). Late Mesozoic basin and range tectonics and related magmatism in southeast China. *Geosci. Front.* 3 (2), 109–124. doi:10.1016/j.gsf.2011.11.007

Wang, J., Cai, Y., Liu, F. Y., Li, Z., Yuan, G. H., Du, Y. G., et al. (2021). Effect of a vacuum gradient on the consolidation of dredged slurry by vacuum preloading. *Can. Geotechnical J.* 58 (7), 1036–1044. doi:10.1139/cgj-2019-0666

Wang, C., Zeng, F., Gao, S., and Yuan, G. (2023). Experimental study on reinforcement of marine clay by artificial hard shell layer composite foundation. *Mar. Georesources and Geotechnol.* 41 (12), 1393–1403. doi:10.1080/1064119x.2022.2144557

Yang, M., Pan, Y., Feng, H., Yan, Q., Lu, Y., Wang, W., et al. (2024). Fractal characteristics of pore structure of longmaxi shales with different burial depths in southern sichuan and its geological significance. *Fractal Fract.* 9 (1), 2. doi:10.3390/fractalfract9010002

Yang, W., Zhang, X., Wang, B., and Ranjith, P. G. (2025). Experimental study on the physical and mechanical properties of carbonatite rocks under high confining pressure after thermal treatment. *Deep Undergr. Sci. Eng.* 4 (01), 105–118. doi:10.1002/dug2.12079

Zhang, R., Cao, J., Cao, Y., and Guo, Z. (2021). "Research on new type of cement-soil piles to reinforce soft soil foundation," in 7th International Conference on Hydraulic and Civil Engineering and Smart Water Conservancy

and Intelligent Disaster Reduction Forum, ICHCE and SWIDR 2021, 391–394. doi:10.1109/ICHCESWIDR54323.2021.9656285

Zhang, J., Zhang, L., Gao, F., Jiang, J., and He, Z. (2024). Effect of particle size distribution on strength and particle breakage of red-bed soil-rock mixture. *J. Eng. Geol.* 32 (05), 1499–1508.

Zhou, S., Wang, B., and Shan, Y. (2020). Review of research on high-speed railway subgrade settlement in soft soil area. *Railw. Eng. Sci.* 28 (02), 129–145. doi:10.1007/s40534-020-00214-x

Zhou, D., Feng, C., Li, L., Zhou, Y., and Zhu, Q. (2020). Reinforcement effect of inclined prestressed concrete pipe piles on an inclined soft foundation. *Adv. Civ. Eng.* 2020 (1), 5275903. doi:10.1155/2020/5275903

Zhu, J., Cao, W., Li, T., Yan, Z., Xu, Q., and Li, J. (2025). Recent advances in application of coal gasification slag in road construction materials. *J. Traffic Transp. Eng. Ed.*, 1–41.

Zhu, H., Ju, Y., Lu, Y., Yang, M., Feng, H., Qiao, P., et al. (2025). Natural evidence of organic nanostructure transformation of shale during bedding-parallel slip. *Geol. Soc. Am. Bull.* 137 (5-6), 2719–2746. doi:10.1130/b37712.1